

Journal of Pakistan Institute of Chemical Engineers



journal homepage: www.piche.org.pk/journal

DOI: https://doi.org/10.54693/piche.05125



Development and Characterization of Lower, Upper, and Inverse Bainite in an Experimental 0.8wt.% C Steel

M. Ishtiaq^{1*}, A. Inam¹, H. Munir¹, S. M. Hadi¹, S.H. Kayani²

Submitted: 06/02/2023, Accepted: 13/03/2024, Published: 15/03/2024

Abstract

In this study, we have successfully developed lower, upper, and inverse bainite morphologies in a 0.8wt.% C steel through a meticulously designed heat treatment process. The steel underwent a precise sequence of thermal treatments, commencing with austenitization at 900 °C for 30 minutes, followed by austempering at temperatures of 400 °C, 480 °C, and 500 °C, each for a duration of 60 minutes. The deliberate adjustment of carbon content to a higher level played a pivotal role in facilitating the intriguing inverse bainitic transformation. Our findings, corroborated by optical microscope, scanning electron microscope and energy dispersive x-ray diffraction analysis, unequivocally validate the successful formation of these unique microstructures. Further insights emerge from the micro-Vickers hardness testing, which reveals the order of hardness among the samples. The upper bainite structure outperforms all, showcasing the highest hardness. Following closely is the enigmatic inverse bainite, trailed by lower bainite. The traditional ferrite-pearlite structure, which has long been a benchmark, lags behind in terms of hardness. This research not only advances our understanding of the bainitic transformations in high-carbon steels but also highlights the potential for tailored material properties for various engineering applications.

Keywords: Heat Treatment, Austempering, Lower Bainite, Upper Bainite, Inverse bainite

1. Introduction:

In recent years, there has been a growing emphasis on the development of multiphase steel structures with enhanced mechanical properties to cater to the ever-increasing demands of various industries, including the production of critical components like camshafts. One of the promising avenues for meeting these stringent requirements involves the deliberate engineering of a bainitic microstructure [1-4] due to its combination of high strength and improved ductility. The term 'bainite' itself, in the context of steel, owes its nomenclature to Dr. Edgar C. Bain, who initially described it as an "acicular

dark etching aggregate" [5]. In a typical bainitic microstructure, bainitic ferrite laths are prominently featured, typically interspersed with phases such as cementite, martensite, or, on occasions, untransformed austenite [6-8]. Bainite, a well-documented transformation in steel metallurgy, exists in two primary forms: upper bainite and lower bainite, each with distinct transformation kinetics and morphologies. As bainitic transformation takes place within an intermediate temperature spectrum, between the reconstructive ferrite/pearlite and the displacive martensite, the morphology and sequence of carbide

Corresponding Author: ishtiaq.imme@pu.edu.pk

¹Institute of Metallurgy and Materials Engineering, University of the Punjab, 54590 Lahore, Pakistan.

² Department of Aluminum, Korea Institute of Materials Science (KIMS), Changwon, South Korea

precipitation within bainite exhibit variation corresponding to the temperature of transformation. Upper bainite forms at higher temperature while the lower bainite forms comparatively at lower temperature ranges. Extensive studies have been conducted to elucidate the intricate details of these transformations, yielding valuable insights into their microstructures and mechanical behavior [9-17].

Hillert [18] proposed a hypothesis analogous to the formation mechanisms of bainite and pearlite, suggesting a third transformation product. This product involves cementite nucleation as the primary event from parent austenite at higher carbon concentrations, specifically in hypereutectoid steels. He termed this transformation product "inverse bainite". Research on inverse bainite has gained momentum in recent years, revealing its potential significance in materials science and engineering [19-22]. While prior investigations have individually delved into the development and characterization of either lower and upper bainite or inverse bainite, there remains a noticeable gap in the literature—a comprehensive study that encompasses the development of all three bainite types (lower, upper, and inverse)

within a single steel composition is conspicuously absent. This research, thus, sets out to address this critical void in our understanding and aims to achieve the simultaneous formation of all three bainite variants within a 0.8 wt.% C steel. Additionally, it endeavors to undertake a comparative study of these bainitic microstructures, shedding light on their respective characteristics, hardness properties, and potential applications. We utilized optical microscopy (OM), scanning electron microscopy (SEM), and energy dispersive X-ray spectroscopy (EDS) to analyze the microstructure and composition of different phases. Through this work, we aim to contribute significantly to the field of material science and metallurgy by unlocking new possibilities for tailored steel microstructures with diverse properties, promising innovative solutions for the manufacturing and engineering sectors.

2. Experimental:

The steel used in this study was produced at Pakistan Steel Mills, Karachi, Pakistan. The chemical composition, presented in Table 1, was determined through analysis using an Optical Emission Spectrometer (The Thermo ScientificTM).

Table 1: Chemical composition (wt.%) of experimental steel.

Elements	C	si	Mn	Ni	As	Zr	Al	Cu	Fe
Wt.%	0.810	0.851	1.44	1.59	0.191	0.153	0.0351	0.0614	93.7

The steel ingots were initially processed by rolling them into plates with a thickness of 10 mm. Subsequently, metallographic samples were meticulously cut into dimensions measuring 10 cubic millimeters, employing a disc cutter. To ensure the cleanliness of the samples, their surfaces underwent a rough grinding process using P100 grade grinding paper, aimed at removing any scale or impurities.

The next step in the experimentation involved the typical heat treatment of the samples. Initially, these samples were tied with Ni-Cr wire for ease of handling. The tied samples were then subjected to an austenization process, where they were heated to a temperature of 900 °C and held at this

temperature for a duration of 30 minutes, within a Muffle furnace. Following this, the samples were rapidly transferred into a salt bath, comprising a mixture of 50% KNO₃ and 50% NaNO₃, and were maintained at temperatures of 400 °C, 480 °C, and 500 °C for a period of 60 minutes. The chosen austempering temperatures were intended to promote the formation of distinct bainite microstructures, encompassing lower, upper, and inverse bainite. The selection of the bainite start (B_s) temperature was determined in accordance with the equations provided by Steven and Haynes [23]. The subsequent cooling process involved removing the samples from the salt baths, allowing them to cool naturally in air. For a visual representation, the heat treatment cycle is shown in Figure 1.

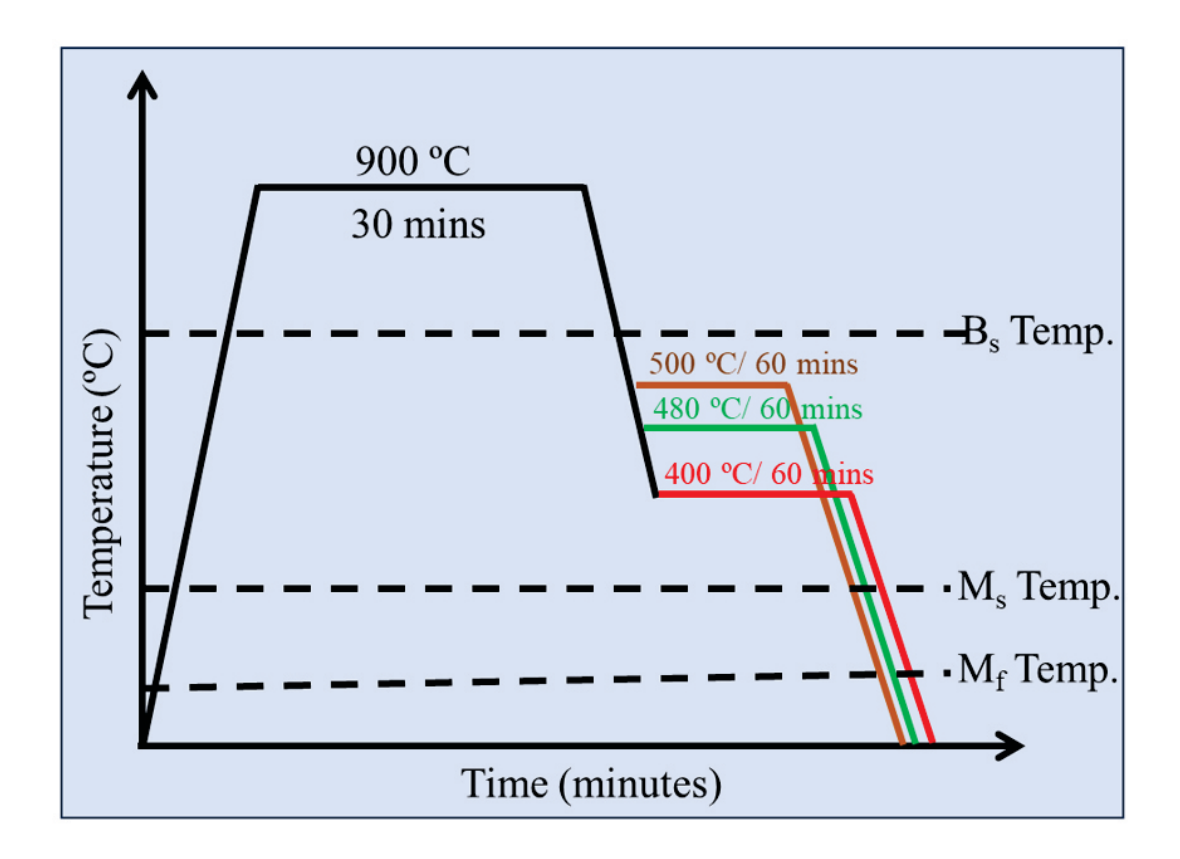


Figure 1: Schematic representation of heat treatment cycle. B_s is bainitic start, M_s is martensitic start and M_t is martensitic finish temperature. Colored lines indicate the austempering temperature and time.

Upon completion of the heat treatment, the samples underwent a cleaning procedure to eliminate any dirt or residual oil from their surfaces. These clean samples were then securely mounted in Bakelite powder using an Automatic Mounting Press (Buehler Brand), to facilitate further analysis. Standard metallographic techniques and practices were meticulously followed to prepare the samples for microscopy. The polished samples were subsequently subjected to an etching process using a 2% Nital solution. To examine the microstructures, OM and SEM were employed. Additionally, spot analysis using EDS was carried out to determine the composition of various spots within the microstructure and identify those specific areas. Finally, the microhardness of the samples was assessed using a Micro-Hardness Tester (Shimadzu Brand). This test was conducted with a minor load of 10 kilograms and a major load of 150 kilograms, providing valuable insights into the hardness characteristics of the material.

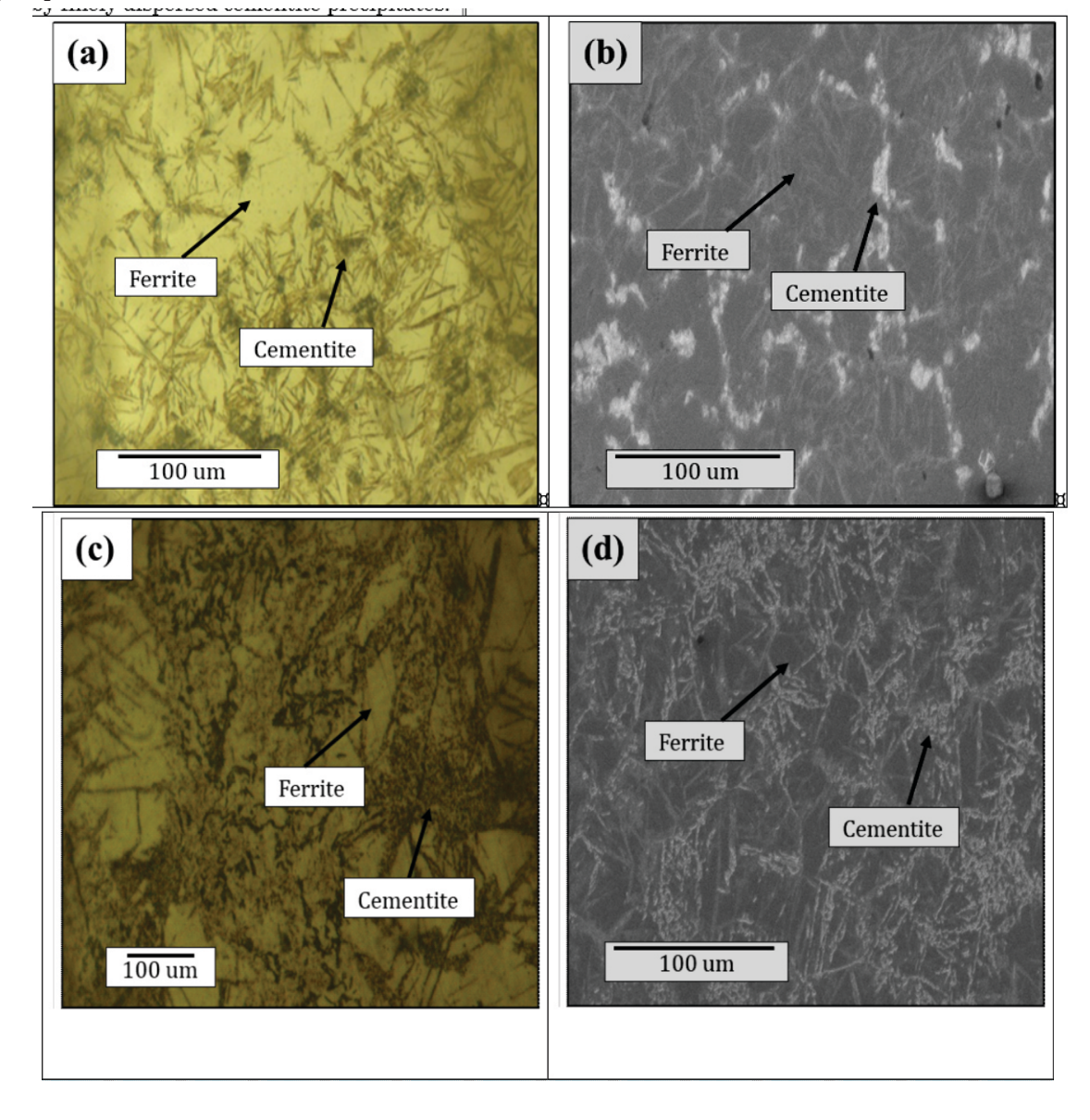
3. Results and Discussion:

3.1 Microstructural Characterization

The austempering heat treatment processes conducted at various temperatures below the B_s temperature effectively induced the transformation of austenite into distinct upper, lower, and inverse bainite structures. This transformation was effectively confirmed through OM and SEM analysis, as depicted in Figure 2. The ferrite (α), with its lower carbon solubility, appears as bright areas in OM images and dark areas in SEM images. Conversely, the carbon-enriched regions, namely cementite (Fe₂C), appear as dark in OM and white in SEM images. Figure 2(a, b) prominently features a typical ferrite-pearlite microstructure, characterized by the coexistence of ferrite and cementite. It is an important observation that despite the higher carbon concentration, the ferrite areas are larger than cementite. This anomaly stems from the abnormal growth of ferrite following the formation of grain boundary cementite. A similar abnormal ferrite phenomenon has been reported in 0.8% C steel [24]. The formation of this abnormal ferrite follows a nucleation and growth mechanism subsequent to the initial formation of pro-eutectoid cementite. Previous studies have demonstrated that this abnormal ferrite can develop on both the allotriomorphic and Widmanstätten forms of the pro-eutectoid cementite and may completely encase the cementite [25].

Figures 2(c, d), however, unveil a distinctive transformation, with cementite diffusing within the ferrite grains, providing unequivocal evidence of lower bainite formation. An evident mechanism for such cementite formation is through the process of precipitation from the ferritic component, which is highly supersaturated within lower bainite. Given

the substantially higher carbon diffusivity in ferrite compared to austenite [26], both the acquisition and retention of sufficient carbon supersaturation to explain the substantial volume fractions of carbides often observed within lower bainite necessitate rapid growth rates of its ferritic component. During the formation of lower bainite, the transformation temperature is relatively low, constraining the effective diffusion of carbon within the microstructure. Consequently, carbon primarily precipitates in the form of cementite but the thickness of cementite precipitation is comparatively thinner. The presence of these slender ferrite-cementite sheaves imparts greater toughness to lower bainite in comparison to upper bainite. The dark appearance of lower bainite plates is attributed to their enhanced etching susceptibility, which is primarily caused by finely dispersed cementite precipitates.



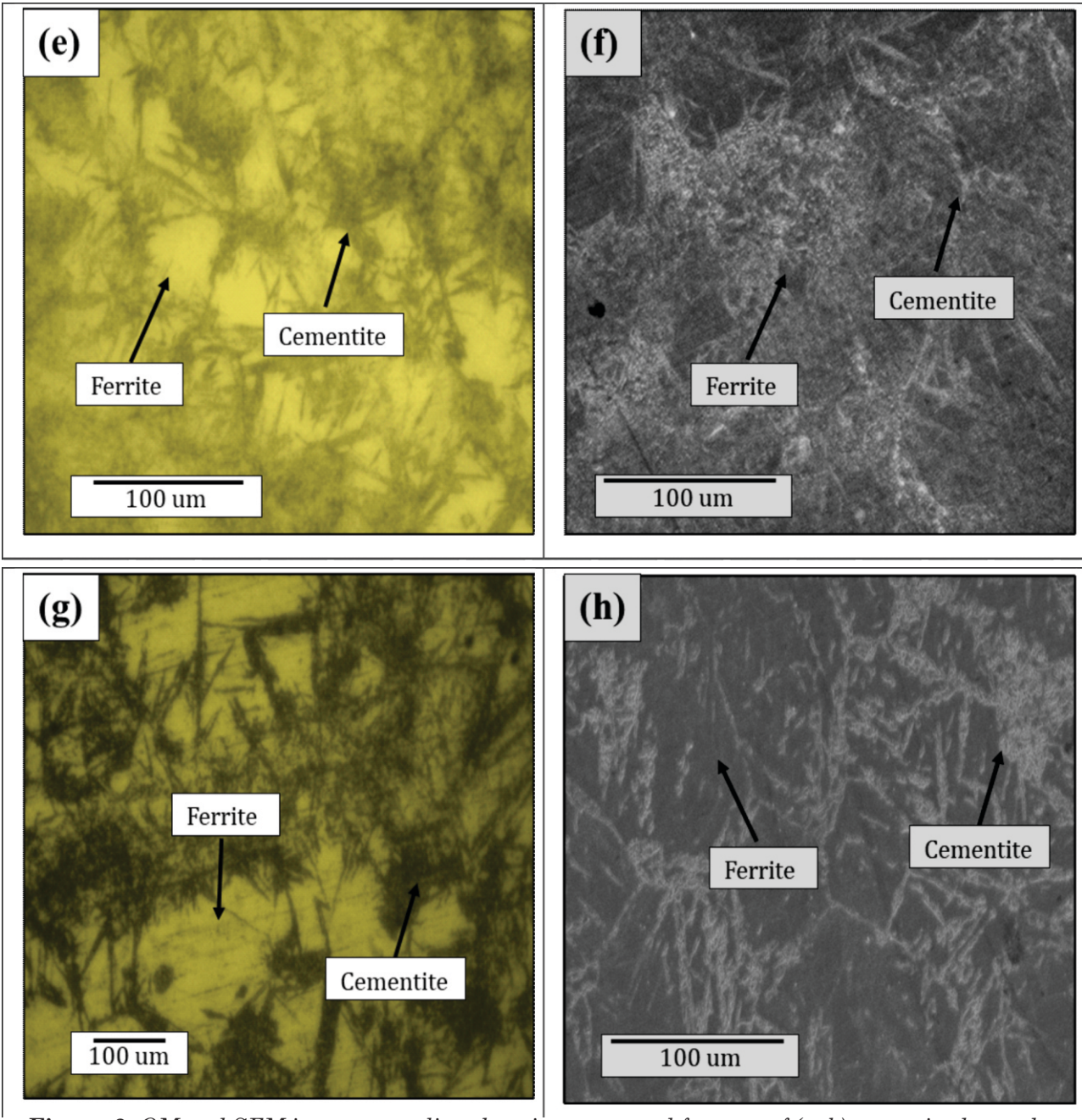


Figure 2. OM and SEM images revealing the microstructural features of (a, b) as-received samples showing typical ferrite-pearlite microstructure (c, d) lower bainite having carbon precipitated inside ferrite (e, f) upper bainite having carbide precipitation at the grain boundaries of ferrite (g, h) inverse bainite showing carbide mid ribs in ferrite.

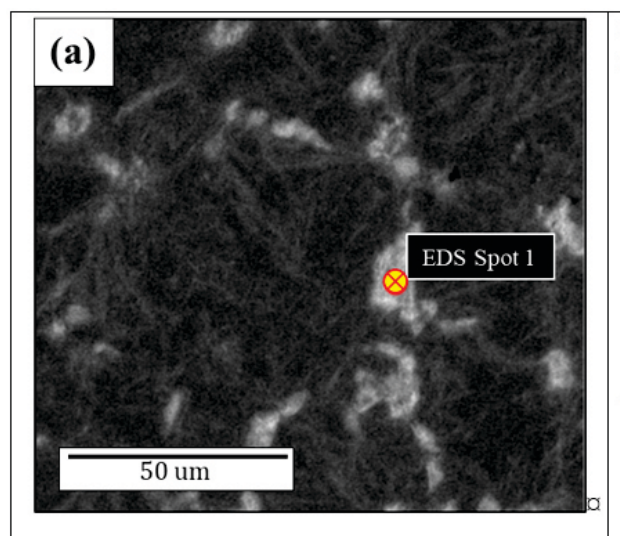
Figures 2(e, f) illustrate the formation of cementite on the boundaries of lath-like ferrite, a characteristic feature of upper bainite [27]. Unlike lower bainite, upper bainite exhibits coarser bainitic ferrites attributed to its higher transformation temperature, which accelerates diffusion kinetics. As ferrite possesses low carbon solubility, excess carbon is rejected, resulting in the formation of cementite at the grain boundaries. The conspicuous thickness of these cementite sheaves contributes to the superior hardness of upper bainite, a characteristic that is corroborated by hardness testing results. In Figure 2(g, h), a microstructure featuring homogeneously dispersed bainitic ferrite and finely distributed needle-like cementite is presented. This particular structure

aligns with the concept of inverse bainite, originally defined by Hillert [18], where cementite serves as the primary nucleating phase. Inverse bainite arises from a series of sequential phase transformations initiated from the parent austenite, resembling the transformation process observed in Widmanstätten ferrite/bainitic ferrite, characterized by carbon diffusion-controlled growth [22]. Previously documented free energy calculations [19] suggest that the free energy change becomes negative when the carbon concentration falls below 0.807%. However, in our steel samples, the carbon concentration slightly exceeds this threshold at 0.810%. Consequently, at this inverse bainitic transformation temperature, the formation of cementite midribs is favoured over the transformation of austenite to ferrite.

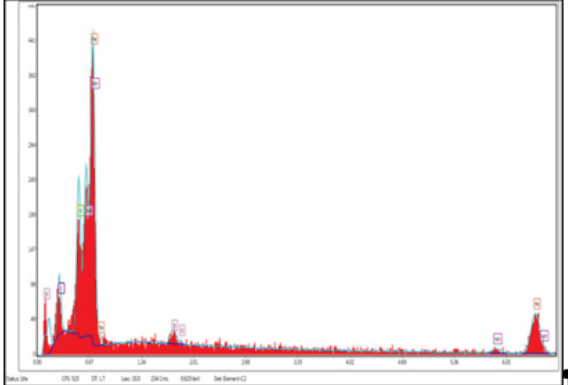
3.2. Phase Identification via SEM-EDS Analysis

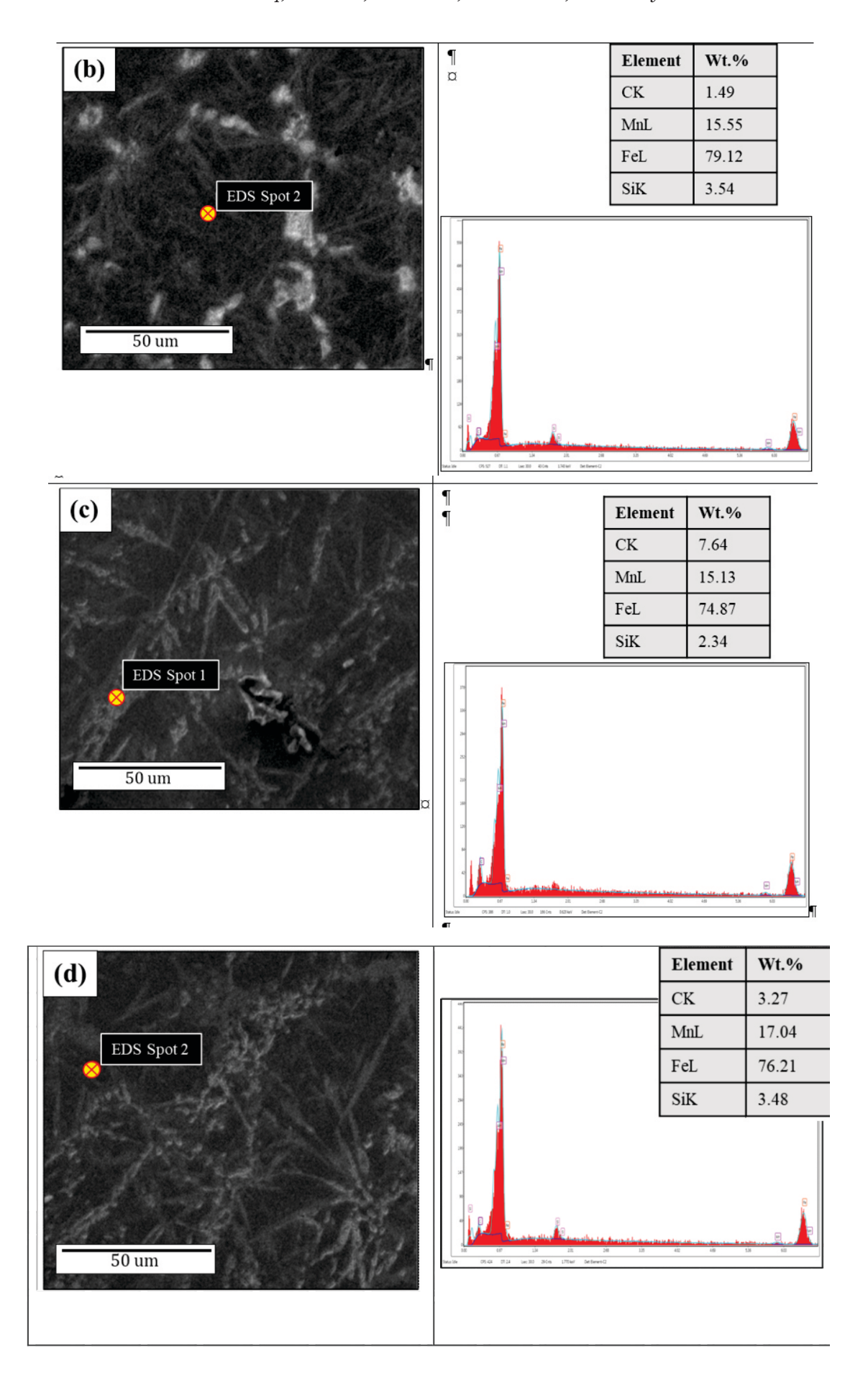
The identification of different phases observed in SEM was carried out by determining their chemical composition using SEM-EDS analysis. The results, indicating whether these phases are ferrite or cementite, are presented in Figure 3. The table corresponding to the EDS spot in the SEM image provides the elemental composition (wt.%) that aids in distinguishing the phase, particularly based on the carbon concentration, as ferrite and cementite exhibit a significant difference in carbon concentration.

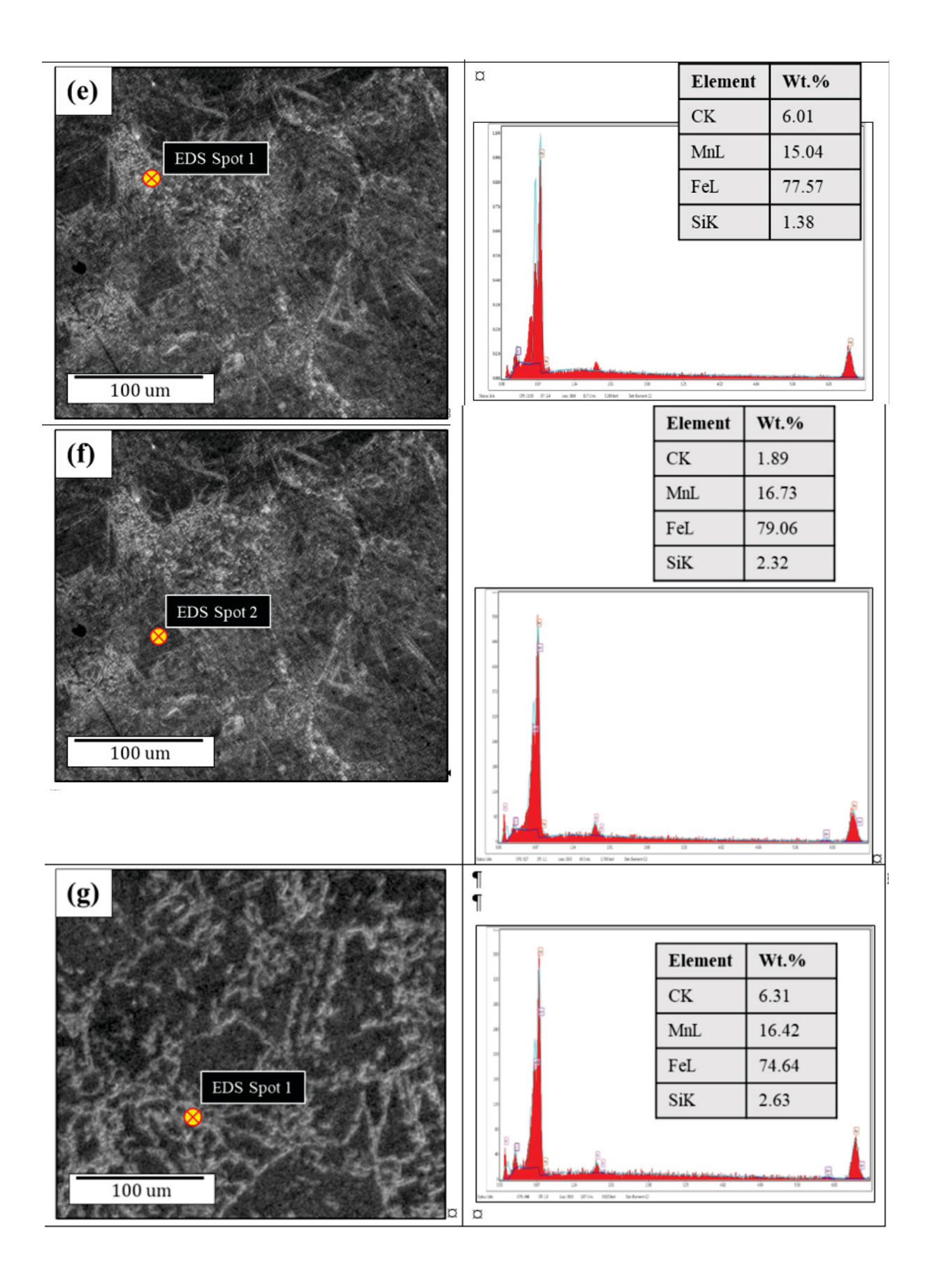
Figure 3(a) reveals that at spot 1, the carbon content is 8.63 wt.%, which aligns more closely with cementite composition compared to ferrite. This confirms the presence of cementite in this area, as the maximum carbon content theoretically permissible within cementite is approximately 6.67%. At spot 2, situated within the dark region in Figure 3(b), the carbon content is measured at 1.49 wt.%, confirming its identity as ferrite. Figure 3(c) showcases another EDS spot analysis, revealing that at spot 1, the carbon content is quantified at 7.64 wt.%, affirming its composition as cementite. Meanwhile, Figure 3(d) demonstrates that at spot 2, the carbon content is determined to be 3.27 wt.%, suggesting its possible affiliation with ferrite.



Element	Wt.%
CK	6.63
OK	11.96
MnL	8.24
FeL	71.04
SiK	2.13







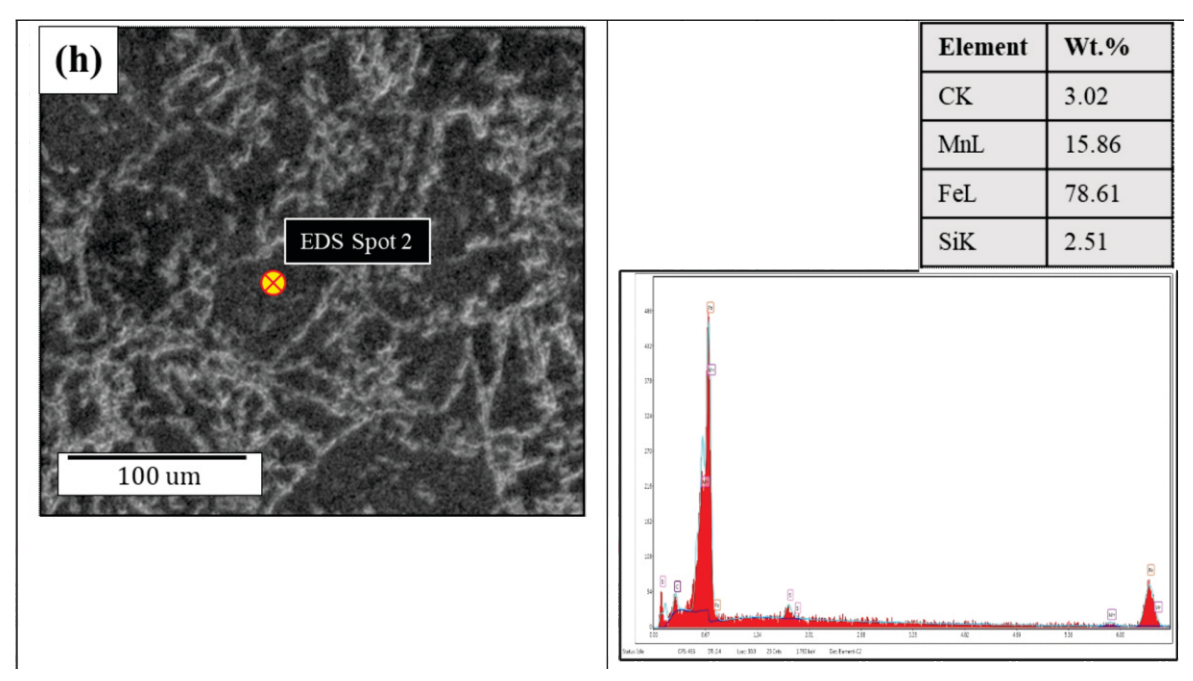


Figure 3. SEM spot EDS spectra of 0.8% C steel (a, b) as received (c, d) lower bainite (e, f) upper bainite (g, h) inverse bainite; inset table gives the composition (wt.%) at the marked point by EDS analysis.

In Figure 3(e), the carbon content at spot 1 for upper bainite is 6.01 wt.%, closely approximating the theoretical carbon content in cementite. Meanwhile, in Figure 3(f), the carbon concentration at spot 2 is 1.89%, confirming it as ferrite. This finding strongly supports the presence of cementite in upper bainite. Similarly, in Figure 3(g) for inverse bainite, the carbon content at spot 1 is measured at 6.31 wt.%, aligning closely with the theoretical carbon content of cementite (6.67 wt.%). This confidently establishes the composition at spot 1 as cementite. In Figure 3(h), the carbon content at spot 2 is measured at 3.02 wt.% C, closely aligning

with the characteristics of ferrite, thus confirming its identity as ferrite.

4. Comparative Hardness Analysis

Figure 4 presents a comparative analysis of the hardness properties between the as-received sample and samples with different developed morphologies of bainite, providing valuable insights into their respective characteristics. The error bars in the graphs represent the variability or uncertainty associated with each hardness measurement, providing a visual representation of the range of possible values around the mean hardness for each sample.

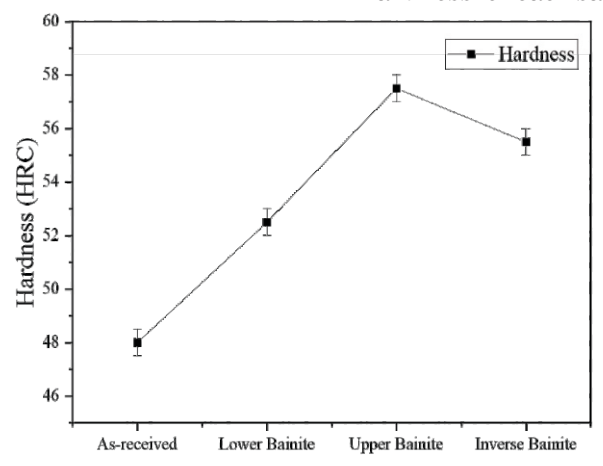


Figure 4: Comparison graph of hardness values of different developed microstructures.

The hardness of upper bainite surpasses that of inverse bainite, lower bainite, and even the asreceived ferritic-pearlitic 0.8% C steel. This notable disparity in hardness can be predominantly attributed to the distinct microstructures formed during the austempering process, with the austempering temperature playing a pivotal role. Upper bainite, developed at a higher temperature of 500 °C, showcases a coarser microstructure, which inherently contributes to its elevated hardness in comparison to the other bainite variants. In contrast, inverse bainite, formed at 480 °C, exhibits slightly lower hardness. Lower bainite, created at 400 °C, demonstrates a characteristic hardness level, while the as-received 0.8% C eutectoid steel, preserved at room temperature, records the lowest hardness among the specimens.

The hierarchy of hardness values within the samples can be summarized as follows:

Upper Bainite > Inverse Bainite > Lower Bainite > As Received (0.8% C).

5. Conclusions:

The following conclusions have been derived from this study:

- 1. Lower, upper, and inverse bainite structures were successfully developed within the 0.8 wt.% C experimental steel.
- 2. In the case of inverse bainite, formed at 480 °C, cementite nucleation started first from parent austenite as cementite midrib followed by ferrite formation which surrounded the cementite midrib.
- 3. Conversely, in lower bainite, which formed at 400 °C, the formation of cementite occurred entirely within ferrite.
- 4. Upper bainite, developed comparatively at higher temperature of 500 °C, exhibited a distinct structure comprising cementite between ferrite laths.
- 5. The highest recorded level of hardness was observed in the upper bainite microstructure, while the lowest hardness was noted in the ferritic-pearlitic microstructure.

References:

- 1 H. Bhadeshia, "Bainite in steels: transformation, microstructure and properties," London: The Institute of Materials, University of Cambridge, pp. 377-382, 2001.
- 2 F. G. Caballero and H. K. D. H. Bhadeshia, "Very strong bainite," Current Opinion in Solid State and Materials Science, vol. 8, no. 3, pp. 251-257, 2004/06/01/2004.
- 3 H. Bhadeshia, "Nanostructured bainite," Proceedings of The Royal Society A: Mathematical, Physical and Engineering Sciences, vol. 466, pp. 3-18, 10/21 2009.
- 4 B. De Cooman, "Structure-properties relationship in TRIP steels containing carbide-free bainite," Current Opinion in Solid State and Materials Science, vol. 8, pp. 285-303, 06/01 2004.
- 5 E. Davenport and E. C. Bain, Transformation of austenite at constant subcritical temperatures. American Institute of Mining and Metallurgical Engineers, 1930.
- 6 R. F. Hehemann, K. R. Kinsman, and H. I. Aaronson, "A debate on the bainite reaction," Metallurgical Transactions, vol. 3, no. 5, pp. 1077-1094, 1972/05/01 1972.
- 7 I. Timokhina, H. Beladi, X. Xiong, Y. Adachi, and P. Hodgson, "Nanoscale microstructural characterization of a nanobainitic steel," Acta Materialia, vol. 59, pp. 5511-5522, 08/01 2011.
- 8 C. Garcia-Mateo and F. Caballero, "Ultrahighstrength Bainitic Steels," ISIJ International, vol. 45, 01/01 2007.
- 9 H. K. D. H. Bhadeshia and D. V. Edmonds, "The mechanism of bainite formation in steels," Acta Metallurgica, vol. 28, no. 9, pp. 1265-1273, 1980/09/01/1980.
- 10 R. WT, H. Aaronson, and G. Spanos, "A summary of the present diffusionist views on bainite," Materials Transactions, JIM,

- vol. 32, no. 8, pp. 737-746, 1991.
- 11 Z.-G. Yang and H.-S. Fang, "An overview on bainite formation in steels," Current Opinion in Solid State and Materials Science, vol. 9, no. 6, pp. 277-286, 2005/12/01/2005.
- 12 L. C. D. Fielding, "The Bainite Controversy," Materials Science and Technology, vol. 29, no. 4, pp. 383-399, 2013/04/01 2013.
- 13 F. G. Caballero, M. K. Miller, C. Garcia-Mateo, and J. Cornide, "New experimental evidence of the diffusionless transformation nature of bainite," Journal of Alloys and Compounds, vol. 577, pp. S626-S630, 2013/11/15/2013.
- 14 H. Chen and S. van der Zwaag, "A general mixed-mode model for the austenite-to-ferrite transformation kinetics in FeCM alloys," Acta Materialia, vol. 72, pp. 1-12, 2014/06/15/2014.
- 15 K. Rakha et al., "On low temperature bainite transformation characteristics using in-situ neutron diffraction and atom probe tomography," Materials Science and Engineering: A, vol. 589, pp. 303-309, 2014/01/01/2014.
- 16 I. B. Timokhina et al., "Growth of bainitic ferrite and carbon partitioning during the early stages of bainite transformation in a 2 mass% silicon steel studied by in situ neutron diffraction, TEM and APT," Journal of Applied Crystallography, vol. 49, no. 2, pp. 399-414, 2016.
- 17 J. Yin, M. Hillert, and A. Borgenstam, "Morphology of Upper and Lower Bainite with 0.7 Mass Pct C," Metallurgical and Materials Transactions A, vol. 48, no. 9, pp. 4006-4024, 2017/09/01 2017.
- 18 M. Hillert, "The role of interfacial energy during solid-state phase transformations," Jernkontorets Annaler, vol. 141, pp. 757-

- 789, 1957.
- 19 R. Kannan, Y. Wang, and L. Li, "Microstructural Evolution of Inverse Bainite in a Hypereutectoid Low-Alloy Steel," Metallurgical and Materials Transactions A, vol. 48, no. 12, pp. 6038-6054, 2017/12/01 2017.
- 20. R. Kannan, Y. Wang, and L. Li, "A thermodynamic study of inverse bainitic transformation," Journal of Materials Science, vol. 53, no. 17, pp. 12583-12603, 2018/09/01 2018.
- 21. R. Kannan, Y. Wang, and L. Li, "A dilatometric analysis of inverse bainite transformation," Journal of Materials Science, vol. 53, no. 5, pp. 3692-3708, 2018/03/01 2018.
- 22. R. Kannan, Y. Wang, J. Poplawsky, S. S. Babu, and L. Li, "Cascading phase transformations in high carbon steel resulting in the formation of inverse bainite: An atomic scale investigation," Scientific Reports, vol. 9, no. 1, p. 5597, 2019/04/03 2019.
- 23. W. Steven, "The Temperature of Martensite and Bainite in Low-alloy Steels," Journal of the Iron and Steel Institute, vol. 183, pp. 349-359, 1956.
- 24. I. Le May, P. Fallon, and J. McCall, "Microstructural Science, Volume 7," 1980.
- 25. T. Chairuangsri and D. V. Edmonds, "Abnormal ferrite in hyper-eutectoid steels," Acta Materialia, vol. 48, no. 7, pp. 1581-1591, 2000/04/19/2000.
- D. Beshers, "Diffusion of interstitial impurities," Diffusion, ASM, Metals Park, Ohio, 1973, 209-240, 1973.27H. K. D. H. Bhadeshia and J. Christian, "Bainite in steels," Metallurgical transactions A, vol. 21, pp. 767-797, 1990.